



## Drip water isotopes in semi-arid karst: Implications for speleothem paleoclimatology



Mark O. Cuthbert<sup>a,b</sup>, Andy Baker<sup>c,\*</sup>, Catherine N. Jex<sup>c,1</sup>, Peter W. Graham<sup>c</sup>,  
Pauline C. Treble<sup>d</sup>, Martin S. Andersen<sup>a,1</sup>, R. Ian Acworth<sup>a,1</sup>

<sup>a</sup> Connected Waters Initiative Research Centre, UNSW Australia, 110 King St, Manly Vale, NSW 2093, Australia

<sup>b</sup> School of Geography, Earth and Environmental Sciences, University of Birmingham, Edgbaston, B15 2TT, UK

<sup>c</sup> Connected Waters Initiative Research Centre, UNSW Australia, Sydney, NSW 2052, Australia

<sup>d</sup> Institute for Environmental Research, Australian Nuclear Science and Technology Organisation, New Illawarra Road, Lucas Heights, NSW 2234, Australia

### ARTICLE INFO

#### Article history:

Received 13 November 2013

Received in revised form 14 March 2014

Accepted 16 March 2014

Available online xxxx

Editor: G.M. Henderson

#### Keywords:

evaporation  
water isotopes  
recharge  
karst  
speleothem  
semi-arid

### ABSTRACT

We report the results of the first multi-year monitoring and modelling study of the isotopic composition of drip waters in a semi-arid karst terrane. High temporal resolution drip rate monitoring combined with monthly isotope drip water and rainfall sampling at Cathedral Cave, Australia, demonstrates that drip water discharge to the cave occurs irregularly, and only after occasional long duration and high volume rainfall events, where the soil moisture deficit and evapotranspiration is overcome. All drip waters have a water isotopic composition that is heavier than the weighted mean annual precipitation, some fall along the local meteoric water line, others trend towards an evaporation water line. It is hypothesised that, in addition to the initial rainfall composition, evaporation of unsaturated zone water, as well as the time between infiltration events, are the dominant processes that determine infiltration water isotopic composition. We test this hypothesis using a soil moisture balance and isotope model. Our research reports, for the first time, the potential role of sub-surface evaporation in altering drip water isotopic composition, and its implications for the interpretation of speleothem  $\delta^{18}\text{O}$  records from arid and semi-arid regions.

© 2014 Elsevier B.V. All rights reserved.

## 1. Introduction

Within-cave monitoring of climate, hydrology and drip water biogeochemistry is recognised by the speleothem paleoclimate research community as being essential to the understanding of speleothem proxy records. Numerous monitoring studies have been reported in recent years, many of which are long-term (for example, Baker and Brunson, 2003; McDonald et al., 2007) and include both monitoring and modelling approaches (for example, Treble et al., 2013). However, to date these research efforts have been mostly focused on understanding processes relevant to temperate, sub-alpine and alpine caves. This bias has been predominantly due to the ease of access of cave sites, and the location of cave research groups, rather than the lack of importance of monitoring studies that would be relevant to speleothem records in semi-arid to arid climates.

The most widely used speleothem paleoclimate proxy is  $\delta^{18}\text{O}$ : originally sourced from precipitation, the speleothem water isotopic composition can be later modified due to interactions in the soil and vadose zones and within the cave. In semi-arid environments, the relationship between rainfall and soil water isotopic composition is relatively well understood thanks to series of field and laboratory studies (Allison, 1982, Allison et al. 1983, 1987; Allison and Hughes, 1983; Barnes and Allison, 1988). The occasional rainfall events in a semi-arid climate will infiltrate the soil, leaving an isotopic signature of the precipitation event. Subsequent evaporation leads to a soil water isotope profile that is exponential in profile and isotopically enriched towards the surface. However, as evaporation is the dominant soil hydrological process, the soil volumetric water content is low as water is lost by evaporation. Therefore, on the occasions where the soil moisture deficit is exceeded and groundwater recharge occurs, it is likely that 'old' and isotopically enriched soil water is volumetrically small compared to the event water, and therefore water infiltrating to the vadose zone is likely to have negligible water isotopic enrichment. In contrast to the relatively well understood

\* Corresponding author.

E-mail address: a.baker@unsw.edu.au (A. Baker).

<sup>1</sup> Affiliated to the National Centre for Groundwater Research and Training, Australia.

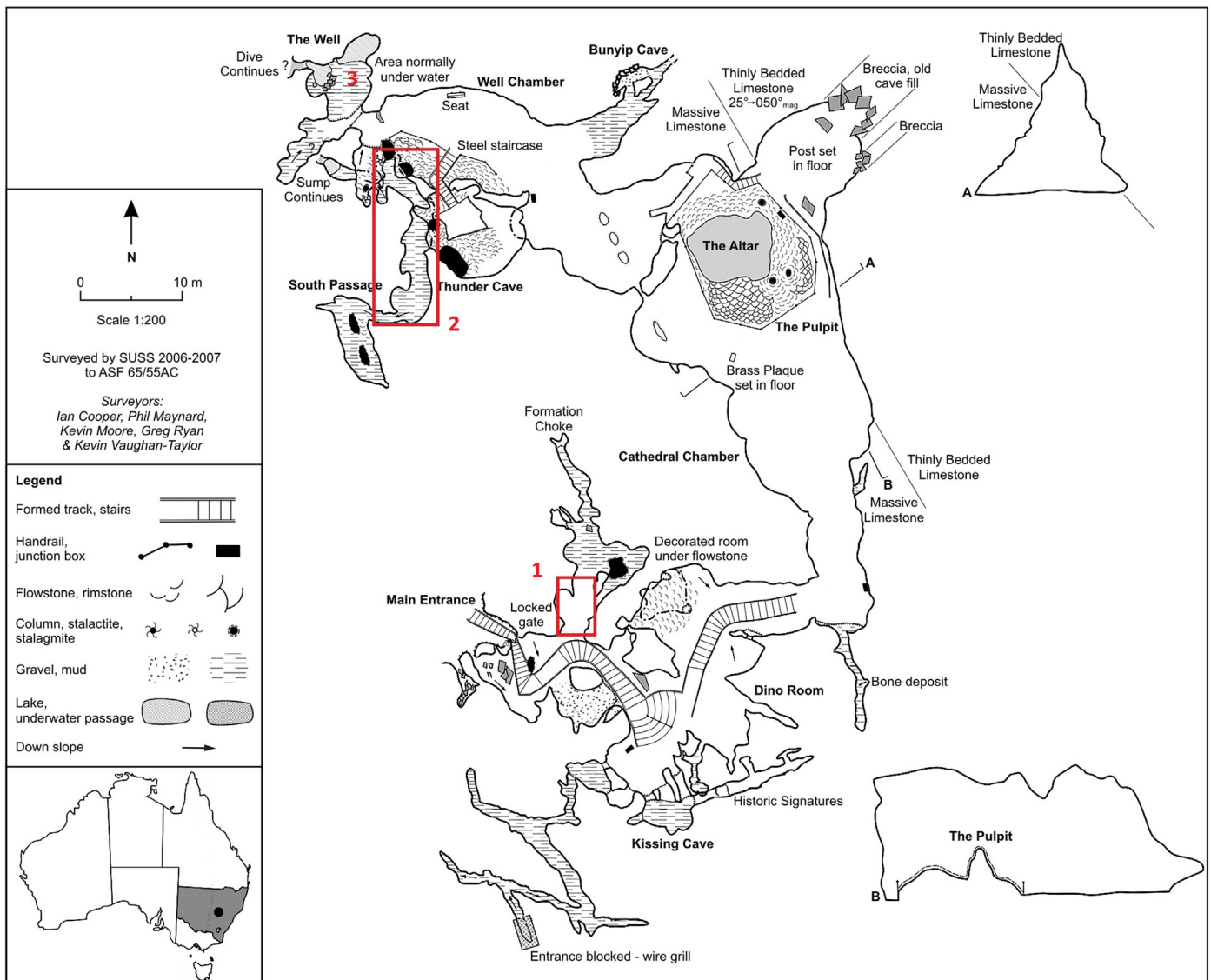


**Fig. 1.** Cathedral Cave sampling locations. Boxes show the two monitoring sites: 1 – the near-entrance site monitoring drip rate and 2 – the the deeper South Passage site monitoring drip rate and drip water isotopes. The locations of monitoring sites at the latter are shown in more detail in Fig. 3c. Also labelled is 3 – groundwater sample location ‘The Well’. The cave survey is reproduced with permission of the Sydney University Speleological Society.

soil water isotope processes, there are almost no studies that have investigated water isotope processes in the vadose zone in semi-arid to arid environments. In karst systems, Ingraham et al. (1990) is a lone study that investigates the water isotopic composition of pool waters in the Carlsbad cave system of New Mexico, USA, to help constrain evaporative water fluxes within the cavern.

Here we report the results of a two-year drip water and rain water isotope monitoring study from Cathedral Cave at Wellington, New South Wales, Australia. Mean annual precipitation is 619 mm (1956–2005) and evaporation is 1825 mm (1965–2005; recorded at the nearby Wellington Research Centre, Australia Bureau of Meteorology). At this site  $ET \gg P$  and so the processes inferred from our monitoring of drip water isotopic composition are most relevant to semi-arid and arid climate regions. Additionally, we utilise the monitoring results to constrain a modified soil moisture balance model. Extending the approach of Cuthbert et al. (2013), we add a soil and groundwater isotope component to understand the processes controlling drip water isotopic composition at our site.

## 2. Methods and site description

### 2.1. Site background

Our monitoring and modelling experiment was undertaken at Cathedral Cave in Wellington, New South Wales, Australia ( $32^{\circ}37'S$ ;  $148^{\circ}56'E$ ) (Fig. 1). The cave entrance, at 325.16 m elevation, is situated close to the top of a north–south trending ridge formed from Devonian Garra Formation limestone. To the west of this ridge, at an elevation of c. 300 m, are the alluvial gravels of the Bell River. The geomorphology of the cave has been extensively researched (Osborne et al., 2007) and is primarily orientated along the direction of jointing ( $150^{\circ}$ ), and contains abundant evidence of hypogene formation processes, arguably typical of many caves in SE Australia (Osborne et al., 2010). The cave descends approximately 25 m from the entrance to the end of the cave, where the cave is flooded as it intercepts the local groundwater at The Well (Fig. 1). Groundwater is observed at an elevation of between 280–300 m asl, depending on antecedent climate conditions. The cave is overlain by degraded box grass woodland, with bare soil and sparse tree cover (Blyth et al., 2014).

Our observations of the cave climatology are consistent with its morphology, which is a descending dead-end cave. Two entrances, located at the same elevation in the entrance series, could lead to limited ventilation in that part of the cave. Air exchange close to the entrance would also be expected through pressure and density effects on both the cave air and groundwater level. Air temperature measurements using Star-Oddi micro loggers show little variation ( $18.25 \pm 0.05$  °C, August 2011 to August 2012) in South Passage (our Site 2, Fig. 1) over the long-term. Near the entrance (Site 1, Fig. 1), we have logged temperature variability over the short term and observe a range of 17–18 °C in January 2013 and 18–23 °C in February 2014. Relative humidity in the cave has been recorded using a Campbell HMP155A over short campaigns and was observed to be constant at 97% at Site 2 (Jan–Feb 2014), consistent with the presence of an adjacent groundwater body, and variable from 73–93% at Site 1, consistent with ventilation within the entrance series. Within cave evaporation has been measured by measuring the volumetric water loss of 50 ml water placed in petri dishes: at Site 1, average evaporation was 0.14 mm/d (over the period 7–15 January 2014) and 0.08 mm/d (from 15 January to 6 March 2014) and at Site 2 was 0.004 mm/d (from 15 January to 6 March 2014).

The cave has been a focus of long-term hydrogeological monitoring by the investigators, commencing in 2009 and continuing, primarily using a network of in-situ Stalagmate © drip loggers. Jex et al. (2012) describe drip water patterns and processes within the cave for a spatially dense network of drip-collection sites: it is a subset of drip waters from this network at Site 2 which are investigated here. Mariethoz et al. (2012) utilised near-surface infiltration to identify non-linear and chaotic drip behaviour and its relationship to surface connectivity. Most recently, and subsequent to the results presented here, at Site 1, we have undertaken an artificial irrigation experiment to better understand infiltration processes (Rutledge et al., 2014).

2.2. Monitoring methods

Our water isotope monitoring program was designed as follows. Monthly integrated rainfall samples were collected using standard IAEA protocols (<http://www-naweb.iaea.org/napc/ih/documents/userupdate/sampling.pdf>) at the nearby (7 km) UNSW Wellington Field Station. Drip water was collected at fifteen monitoring sites within the South Passage of Cathedral Cave (Site 2, Fig. 1); five (sites 279, 280, 372, 395 and 396) were part of the network described by Jex et al. (2012). Isotope water samples were collected via funnels connected to 500 ml or 1 l HDPE bottles. Paraffin was placed in the bottles as a precaution to prevent evaporation within the bottles. Evaporation could be possible anywhere prior to collection, although our within-cave relative humidity measurements suggest that this is unlikely to occur within the cave at Site 2. Bottles were changed monthly, with fresh paraffin added, and an integrated 30 ml water sample transferred to sealed glass McCartney bottles with no headspace to prevent evaporation whilst in storage. These bottles were then stored until analysis, which occurred within two months. Water samples were collected at monthly intervals from March 2011 to March 2013.

Drip rates were monitored using a network of twenty-six Stalagmate © drip loggers in South Passage (Site 2) and a further four drip loggers situated closer to the surface (Site 1, including site 326 of Jex et al., 2012). This is the expanded network referred to by Jex et al. (2012). Our intention was to measure the infiltration rate using Stalagmate © drip loggers for all isotope sample sites, but our monthly sampling frequently disturbed the drip logger alignment, and only seven of our fifteen isotope sample sites had reliable drip data. Drip rate data are presented in Table 1, together with a classification of the drip type (soda straw stalactite; non-soda straw stalactite, non-soda straw stalactite underneath flowstone).

**Table 1** Drip water and local river and groundwater isotopic composition. For each drip site, a 'drip water line' and its correlation coefficient is shown, along with the standard error of both gradient (M) and intercept (C). Drip types are classified as soda straw stalactite (So), non-soda-straw stalactite (St) and non-soda-straw stalactite within flowstone (F).

Site ID	Drip type	Mean (drips/15 min)	Median (drips/15 min)	Maximum (drips/15 min)	$\delta^{18}\text{O}$		$\delta^2\text{H}$		$\delta^2\text{H} = M * \delta^{18}\text{O} + C$			r	
					mean	sd	mean	sd	M	C	N		
279	St	8.28	1.00	368.00	-2.81	0.84	-10.52	6.75	7.03	0.81	9.22	2.38	0.88
280	So	0.89	1.00	3.00	-2.50	0.78	-7.38	6.18	6.85	0.82	9.76	2.13	0.87
319	So	1.85	2.00	14.00	-3.45	0.38	-17.72	1.99	3.08	0.92	-7.08	3.21	0.59
320	St	3.04	0.00	110.0	-2.43	1.16	-6.53	9.42	7.54	0.62	11.81	1.67	0.93
322	So	0.32	0.00	3.00	-1.98	0.91	-3.08	5.76	5.00	0.87	6.85	1.88	0.79
330	St	nd	nd	nd	-2.62	0.90	-9.84	6.10	4.49	0.86	5.47	2.36	0.81
368	So	nd	nd	nd	-2.90	0.71	-13.42	5.06	5.91	0.82	3.74	2.45	0.83
372	F	0.36	0.00	2.00	-2.36	0.90	-7.82	6.94	6.91	0.74	8.51	1.85	0.90
380	So	nd	nd	nd	-2.88	0.84	-12.85	5.34	5.23	0.88	2.24	2.63	0.82
382	F	nd	nd	nd	-1.96	0.98	-4.51	6.72	6.09	0.67	7.39	1.45	0.89
387	So	nd	nd	nd	-2.24	1.03	-6.13	7.70	6.90	0.73	9.33	1.80	0.92
395	So	3.90	3.00	11.00	-2.76	0.64	-12.43	4.79	5.90	0.99	3.84	2.79	0.79
396	St	nd	nd	nd	-1.16	0.73	-1.16	4.62	4.63	1.05	5.83	1.74	0.73
398	So	nd	nd	nd	-2.19	0.96	-7.06	7.63	7.47	0.63	9.33	1.49	0.94
UK1	St	nd	nd	nd	-3.30	0.75	-16.71	5.79	6.45	0.98	4.54	3.31	0.83
RAIN					-4.28	2.18	-23.54	16.48	7.29	0.43	7.68	2.08	0.96
Rivers													
MACQUARIE					-4.27	0.75	-24.58	3.06					
BELL					-4.45	0.59	-26.24	3.68					
Groundwater													
ANTICLINE					-4.43	0.53	-25.50	1.44					
WELL					-4.46	0.44	-26.41	2.34					

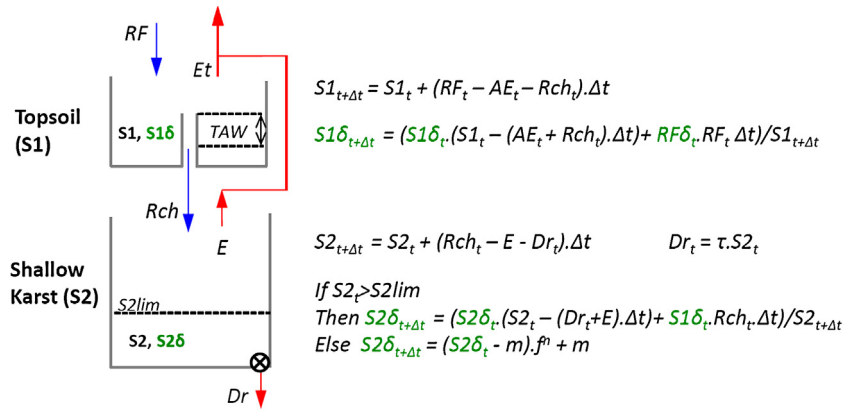


Fig. 2. Schematic illustration of the modelled processes. Variables are all defined in the main text.

Water isotopic composition of drip water and rainwater samples was determined using an LGR-24 d off-axis, integrated cavity output, cavity ringdown mass spectrometer (ICOS CRMS, Lis et al., 2007; Wassenaar et al., 2008) at the University of New South Wales. Five internal reference standards (LGR#1 to LGR#5, with  $\delta^{18}\text{O}$  values of  $-19.5\text{‰}$ ,  $-16.14\text{‰}$ ,  $-13.1\text{‰}$ ,  $-7.69\text{‰}$ ,  $-2.8\text{‰}$ ) and one external reference standard (VSMOW2,  $0\text{‰}$ ) was analysed as an external standard; and during the analysis period we participated in the 4th IAEA Inter Laboratory Comparison for stable isotopes of water (WICO2011, laboratory 082). Two samples analysed were outside the range of the  $\delta^{18}\text{O}$  standards, but by less than the analytical precision. Analytical precision for  $\delta^{18}\text{O}$  was  $0.17\text{‰}$  for  $\delta^{18}\text{O}$  and  $0.6\text{‰}$  for  $\delta^2\text{H}$  ( $1\sigma$ ; calculated from within run internal references materials).

### 2.3. Modelling methods

A model was developed to simulate groundwater recharge, shallow karst flow and isotopic composition of drip waters at the field-site and is illustrated schematically in Fig. 2. A soil moisture balance (SMB) model was used for the topsoil which, based on Cuthbert et al. (2013), makes use of a combined crop co-efficient approach ( $K_c$ ) taken from Allen et al. (1998). The total available water (TAW) in the soil is defined as:

$$TAW = (\vartheta_{FC} - \vartheta_{WP}) \cdot Z_r \cdot (1 - B) + (\vartheta_{FC} - 0.5\vartheta_{WP}) \cdot Z_e \cdot B \quad (1)$$

where  $\vartheta_{FC}$  &  $\vartheta_{WP}$  are fractional soil moisture contents at field capacity (FC) and wilting point (WP),  $Z_r$  is the rooting depth of crop,  $Z_e$  is the thickness of the soil layer subject to drying by evaporation,  $B$  = fractional area of bare soil (i.e. crop absent). The readily available water (RAW) is defined as:

$$RAW = p \cdot TAW \quad (2)$$

where  $p$  is a factor normally between 0.2 and 0.7 (Allen et al., 1998, Table 22). If the soil moisture deficit in the topsoil ( $SMD_s$ ) is greater than the RAW then the actual evaporation rate ( $AE$ ) is reduced using a stress co-efficient ( $K_s$ ) as follows:

$$AE = K_s PE \quad (3)$$

$$K_s = (TAW - SMD_s) / (TAW - RAW) \quad (4)$$

where potential evapotranspiration,  $PE = K_c PE_0$  and  $PE_0$  is the reference crop (grass) potential evapotranspiration rate.

Using a daily input time series for rates of rainfall ( $RF$ ) and  $PE_0$ , the model algorithms calculate time series of  $AE$  and the rate of groundwater recharge ( $Rch$ ). Overland flow is very rare at the field site and has therefore been assumed to be zero with all rainfall ( $RF$ ) becoming infiltration. On days where the soil is under

stress and rainfall occurs that is less than  $PE$  the rainfall is transpired plus a further amount from the soil equal to the remaining evaporative demand modified by the stress co-efficient. If rainfall exceeds the  $PE$  then the excess reduces the  $SMD$  and once this has become zero any additional excess becomes groundwater recharge.

Continuous time-series of potential evapotranspiration ( $PE_0$ ) and rainfall were obtained from nearby continuous automatic weather stations at the caves (Hill Station, operational from November 2011) and UNSW Research Station (operational until damaged by bushfire in December 2012) and the daily Bureau of Meteorology (BOM) station in Wellington (Station Number: 65034, located at Wellington Agrowplot (lat:  $32.56^\circ\text{S}$ /Long:  $148.95^\circ\text{E}$ /350 m asl), 6.5 km from the caves). For the rainfall data, double mass plots were derived for the three site combinations and the linear correlations used to infill missing data from the Hill Station.  $PE_0$  was calculated using the Penman–Montieth reference crop evapotranspiration using the UNSW Research Station data and a pan factor was derived from the BOM Station using a linear relationship between the two. Where data gaps persisted, the correlation between average monthly temperature and average monthly  $PE_0$  was used for filling data gaps.

To estimate the drip water  $\delta^{18}\text{O}$  composition reaching the cave monitoring points, rainfall events were assigned isotopic compositions based on the measured monthly values and the soil store was assumed to be fully mixed. The soil store ( $S1$ ) evolved through time ( $t$ , in increments of  $\Delta t = 1$  day) according to the following mass balance equation:

$$S1_{t+\Delta t} = S1_t + (RF_t - AE_t - Rch_t) \cdot \Delta t \quad (5)$$

where  $S1_t$  and  $S1_{t+\Delta t}$  is the amount of water in the soil store ( $S1$ ) in mm at times  $t$  and  $t + \Delta t$  respectively. Using the suffix  $\delta$  to represent  $\delta^{18}\text{O}$  isotopic compositions (per mil), the soil store isotopic composition was governed by the following equation:

$$S1\delta_{t+\Delta t} = (S1\delta_t \cdot (S1_t - (AE_t + Rch_t) \cdot \Delta t) + RF\delta_t \cdot RF_t \Delta t) / S1_{t+\Delta t} \quad (6)$$

where  $S1\delta_{t+\Delta t}$  and  $S1\delta_t$  are the isotopic compositions of the soil store ( $S1$ ) at time  $t$  and  $t + \Delta t$  respectively and  $RF\delta_t$  is the isotopic composition of the rainfall at time  $t$ .

The model does not include isotopic fractionation in the soil zone for two reasons. First, at our site, recharge is erratic and comes from infrequent, large events, typical of arid and semi-arid environments. The soil is typically relatively dry before a recharge event, and even though prior soil water is likely to be enriched in heavy isotopes (Barnes and Allison, 1988), it is volumetrically very small compared to event water. Thus, during an event the residual isotopically enriched water is greatly diluted, the resulting soil

isotopic concentration is very close to that of the incoming meteoric precipitation and this prior soil water cannot be used as a tracer of water movement (Sonntag et al., 1985). The second reason for not including fractionation in the soil zone in the model is that our field data (see Section 3.2) shows that the predominant fractionation process occurs under high humidity. This cannot be accounted for by in-soil evaporation processes in unsaturated soils, where near surface evaporation results in fractionation with the slope of the  $\delta D$ – $\delta^{18}O$  relationship typically  $<4$  (Allison et al., 1983; Barnes and Allison, 1988).

The attenuation and isotopic evolution of the groundwater due to evaporation was then modelled by using the second store ( $S_2$ ,  $S_2\delta$  with initial values  $S_{20}$  and  $S_{2\delta_0}$  respectively). This filled from above with water leaving the soil as groundwater recharge, lost mass due to evaporation which was assigned a constant value, and drained exponentially using a recession constant ( $\tau$ ) to simulate drip water volume and  $\delta^{18}O$  to the deeper karst system ( $Dr$ ,  $Dr\delta$ ) as follows:

$$S_{2t+\Delta t} = S_{2t} + (Rch_t - E - Dr_t) \cdot \Delta t \quad (7)$$

with

$$Dr_t = \tau \cdot S_{2t}. \quad (8)$$

The isotopic composition of the karst store (and any water leaving the store to become drip water) was assumed to be governed by a simple mass balance if the depth of water in the store was greater than a threshold value ( $S_{2lim}$ ):

$$S_{2\delta_{t+\Delta t}} = (S_{2\delta_t} \cdot (S_{2t} - (Dr_t + E) \cdot \Delta t) + S_{1\delta_t} \cdot Rch_t \cdot \Delta t) / S_{2t+\Delta t} \quad (9)$$

However, if  $S_{2t} < S_{2lim}$  then it was assumed, following Confiantini (1986, Eq. (7), p. 117), that an evaporative process in the shallow karst was of the form as follows:

$$S_{2\delta_{t+\Delta t}} = (S_{2\delta_t} - m) \cdot f^n + m \quad (10)$$

Where  $m$  and  $n$  are empirical constants to be determined from model calibration, and  $f$  is the proportion of water left in the store since the level fell below the threshold amount.

Rather than producing a calibrated model for each drip site with different parameters, our approach was rather to attempt to match the range of observed isotopic values with the purpose of testing our conceptual model and providing estimates of the range of model parameter combinations. The SMB flow model was first tuned to capture the overall timing of the main drip events monitored in South Passage by varying the SMB parameters; it was not attempted to match the volume of drip water leaving the karst store against the measured drip data since the distribution of recharge through the karst network is extremely complex and highly variable across all drip sites. This stage of the model refinement was carried out manually since no single objective function could reasonably be defined against which to automate the calibration. For the estimation of parameters for the isotope model we applied a method similar to the widely used GLUE methodology (Beven and Binley, 1992) as follows. The aggregated modelled monthly drip water composition was compared directly against the range of measured values assuming drip water is all sourced from a single shallow store (albeit at different rates) by varying the parameters controlling the karst store and fractionation process. Sets of prior parameter distributions (ranges of estimated initial values) were defined based on physical plausibility and initial experimentation with the model to ensure a wide enough spread to avoid unwanted rejection of any physically plausible parameter sets. Monte Carlo simulations were carried out for 50 000 random combinations of the prior parameter distributions. If all modelled

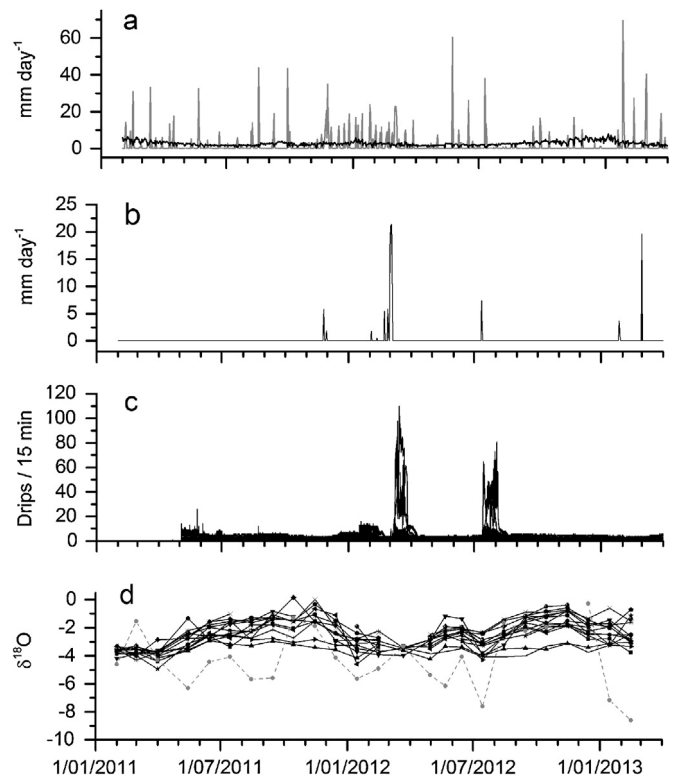


**Fig. 3.** (a) Rainfall (grey line) and potential evaporation (black line); (b) modelled groundwater potential recharge; (c) drip rate for all Stalagmate drip loggers over the study period; (d) rainfall (dashed line) and drip water (solid line) monthly isotope samples.

values fitted within the range of the measured isotopic composition of the drip water across all samples for a given time step this model was deemed ‘behavioural’ and these models were retained (henceforth: physically plausible models). The parameter values of these physically plausible models were used to define the posterior parameter distributions.

### 3. Results and discussion

#### 3.1. Rainfall, evapotranspiration, and drip rates

Rainfall, calculated  $PE_0$  and drip water data for the two-year period are presented in Fig. 3. Average rainfall and  $PE_0$  for Feb 2011 to Feb 2013 are 666 and 982 mm/yr, higher and lower than the long term average respectively, reflecting the slightly cooler and wetter conditions experienced during the monitoring period where La Nina or neutral conditions prevailed. Drip rates are observed to be highly episodic, with only a few rainfall events of high duration and amount resulting in recharge and thus exfiltration in the cave. Drip water responses within the cave show significant variability between sites, as previously demonstrated by Jex et al. (2012). Particularly large drip rates, sometimes over 100 drips per 15 min (equivalent to  $\sim 1 \times 10^{-5} \text{ l s}^{-1}$ ), were observed during Jan–Mar 2012 and Jul–Aug 2012 with periods in between of much slower exfiltration ranging from 0 to approx. 10 drips per 15 min ( $\lesssim 1 \times 10^{-6} \text{ l s}^{-1}$ ).

#### 3.2. Water isotopes

The  $\delta^{18}O$  and  $\delta^2H$  composition of monthly integrated drip water and rainfall samples are summarised in Table 1, and  $\delta^{18}O$  time-series plotted in Fig. 3. Fig. 4 presents the plot of  $\delta^2H$  vs.  $\delta^{18}O$ : also presented on this plot are monthly grab samples collected from adjacent rivers (open squares) and ground water (open circles). River

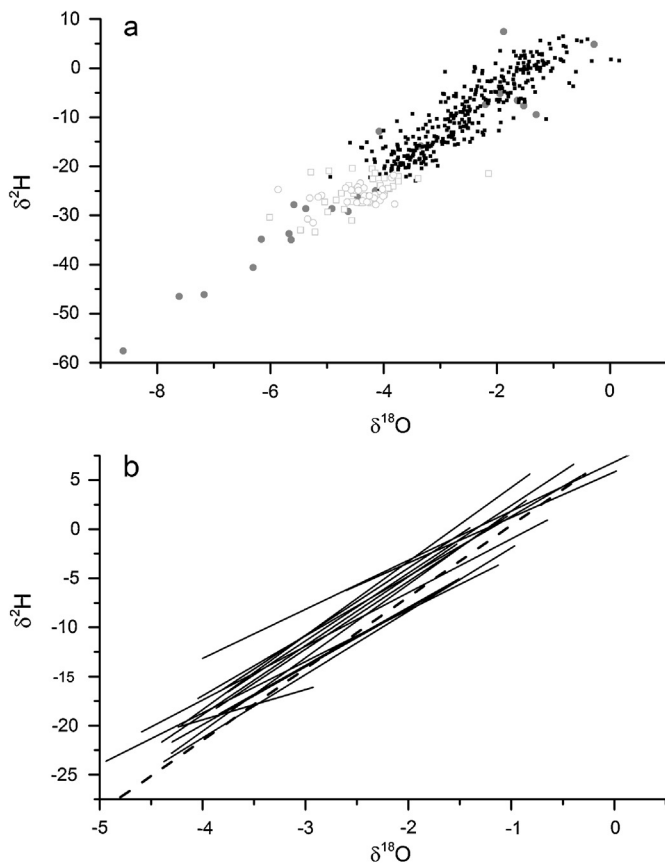


**Fig. 4.** (a)  $\delta^2\text{H}$  vs.  $\delta^{18}\text{O}$  for monthly rainfall (closed circles) and infiltration (small closed squares). Local river water samples (open squares) and groundwater samples (open circles) are also presented. (b) Trend lines of the data presented in (a): Local Meteoric Water Line (dashed line) and  $\delta^2\text{H}$  vs.  $\delta^{18}\text{O}$  regressions for each drip water site (solid lines). Regression equations and correlation coefficients are presented in Table 1.

samples were obtained from the Macquarie River at the UNSW Research Station (7 km to the north–east of the caves) and the Bell River (2 km downstream of the Wellington Caves). Ground water samples were collected within the Wellington Caves Reserve, from Anticline Cave (200 m west of the cave entrance) and from ‘The Well’ in Cathedral Cave (shown in Fig. 1).

Fig. 4 demonstrates that the monthly rainfall samples fall along a local meteoric water line (LMWL) with an equation  $\delta^2\text{H} = 7.29\delta^{18}\text{O} + 7.68$  ( $r = 0.96$ , standard error of the slope = 0.43, standard error on the intercept = 2.08). The annual weighted mean isotopic composition of rainfall over the monitoring period was  $-4.28\text{‰}$  for  $\delta^{18}\text{O}$  and  $-23.54\text{‰}$  for  $\delta^2\text{H}$ , and the river and ground water grab samples all had a mean isotopic composition that reflected the weighted mean of precipitation (Table 1). In contrast, the drip water mean  $\delta^{18}\text{O}$  and  $\delta^2\text{H}$  composition ranged from  $-1.51\text{‰}$  to  $-3.45\text{‰}$ , and  $-1.16\text{‰}$  to  $-17.72\text{‰}$ , respectively. Mean drip water isotopic compositions were therefore 0.83 to 2.77 $\text{‰}$  ( $\delta^{18}\text{O}$ ) and 5.82 to 22.38 $\text{‰}$  ( $\delta^2\text{H}$ ) heavier than the weighted mean annual precipitation.

We observe no relationship between drip water isotopic composition and hydrological properties such as the drip source classification, or drip rate (at the sites where that data is available) (Table 1). Comparing drip source classifications to drip water oxygen isotopic composition, soda-straw ( $n = 8$ ) and non-soda straw ( $n = 5$ ) stalactite drip sources have mean isotopic compositions that are statistically similar (students  $t$ -test, 95% confidence level). Comparing mean, median and maximum drip rates to oxygen isotopic composition, for the drip sites where data is available ( $n = 7$ ),

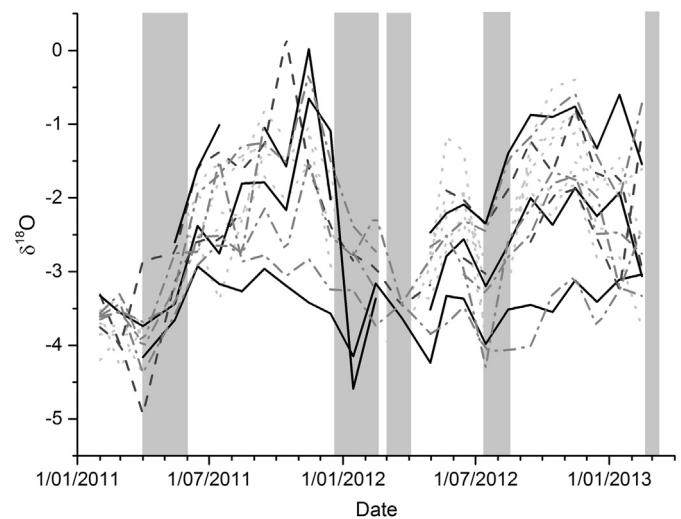


**Fig. 5.** Water  $\delta^{18}\text{O}$  isotope time series shaded by slope of  $\delta^2\text{H}$  vs.  $\delta^{18}\text{O}$  regression.  $>6.8$ , light grey dotted lines;  $6.8\text{--}5.8$ , grey dash-dotted lines;  $5.8\text{--}4.8$ , dark grey dashed line;  $<4.8$ , black solid lines. Solid grey shading represents the periods of recharge (Fig. 2c).

gave slopes of the  $\delta^{18}\text{O}$  vs. drip rate relationship not significantly different from zero.

Typically, from a theoretical perspective, the presence of a water isotopic composition that is heavier than the weighted mean of precipitation would be expected to be due to evaporation of lighter isotopes. The relative enrichment of  $\delta^2\text{H}$  to  $\delta^{18}\text{O}$  varies with the processes that determine evaporative enrichment: the relative humidity and turbulence of the overlying air mass (Confiantini, 1986). In environments with limited air movement, the relative humidity can approach 100%; the slope of the  $\delta^2\text{H}$  vs.  $\delta^{18}\text{O}$  regression will increase and the maximum amount of enrichment decreases with increasing relative humidity. Following Confiantini (1986), in environments with relative humidity larger than 95% the slope of the  $\delta^2\text{H}$  vs.  $\delta^{18}\text{O}$  regression will be similar to that of the LMWL with an enrichment of up to 4 $\text{‰}$  in  $\delta^{18}\text{O}$  possible. In environments with a lower humidity, the slope of the  $\delta^2\text{H}$  vs.  $\delta^{18}\text{O}$  regression decreases, and the maximum amount of enrichment will be greater. Applying this theory to our results, Fig. 4 demonstrates that drip waters as a whole scatter along the LMWL. However, considering each drip site individually, some sites have a slope of the  $\delta^2\text{H}$  vs.  $\delta^{18}\text{O}$  regression that is, within the standard error uncertainty (Table 1), the same as the slope of the  $\delta^2\text{H}$  vs.  $\delta^{18}\text{O}$  regression of the LMWL, indicative of evaporation in a high humidity environment. Others which have a lower slope of the  $\delta^2\text{H}$  vs.  $\delta^{18}\text{O}$  regression than the LMWL, which could be attributed to evaporative enrichment in a less humid environment. Individual regression data is presented in Table 1.

In order to investigate these data further, Fig. 5 presents the  $\delta^{18}\text{O}$  isotopic composition against time for drip sites grouped by their slopes of the  $\delta^2\text{H}$  vs.  $\delta^{18}\text{O}$  regression. Sites which have a similar  $\delta^2\text{H}$  vs.  $\delta^{18}\text{O}$  slope to the LMWL (slope of the  $\delta^2\text{H}$  vs.  $\delta^{18}\text{O}$  regression  $>6.8$ ; sites 279, 280, 320, 372, 387 and 398) have very similar time series. It is also notable that there is no relationship between the rainfall isotopic composition (Fig. 3) and the way drip water isotopes vary during periods of no recharge. Sites which have the lowest slopes of  $\delta^2\text{H}$  vs.  $\delta^{18}\text{O}$  (slope of the  $\delta^2\text{H}$  vs.  $\delta^{18}\text{O}$  regression  $<4.8$ ; sites 319, 322, 330, 380, 396) also have similar time series. However, this group has greater isotopic variability between sites, with some having a wider range towards heavier isotopic compositions. Notably, when comparing the slope of individual  $\delta^2\text{H}$  vs.  $\delta^{18}\text{O}$  regressions vs. mean isotopic composition, no relationship was observed, but a strong correlation is present between the slope of the  $\delta^2\text{H}$  vs.  $\delta^{18}\text{O}$  regression and its

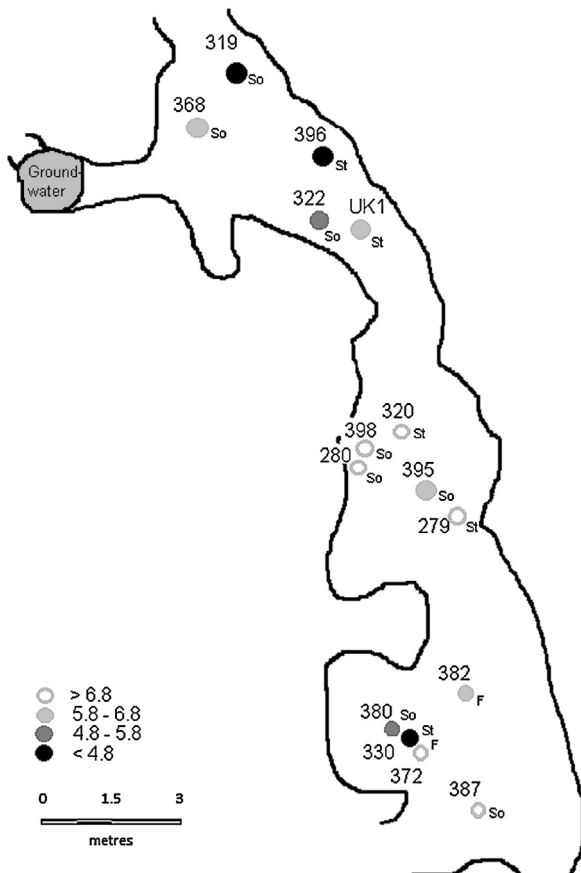


**Fig. 6.** Spatial distribution of Site 2 water isotope samples: see inset, Fig. 1 for location within Cathedral Cave. Site ID and drip classification are as presented in Table 1. Shading and fill of the symbols shows the slope of  $\delta^2\text{H}$  vs.  $\delta^{18}\text{O}$  regression as presented in Table 1.

correlation coefficient ( $r = 0.92$ ). Sites with a steeper slope (e.g. that fall on the LMWL) have the strongest correlation between  $\delta^2\text{H}$  vs.  $\delta^{18}\text{O}$ ; sites with a lower slope have the weakest correlation between  $\delta^2\text{H}$  vs.  $\delta^{18}\text{O}$ .

Inspection of Figs. 4 and 5 demonstrates that the drip sites can be interpreted in the following way:

**Type 1.** Some sites have variable  $\delta^{18}\text{O}$ ,  $\delta^2\text{H}$  vs.  $\delta^{18}\text{O}$  slopes  $> 6.8$  and similar to the LMWL, and very similar time-series. Some sites have discontinuous dripping, with drip flow commencing after the high rainfall events, and the isotopic composition of this initial drip water varies between events. The isotopic composition of the water subsequently becomes heavier during drip flow recession periods. A conventional explanation would be that the drip water comes from a single water source. Isotopic enrichment must occur in this source, and the  $\delta^2\text{H}$  vs.  $\delta^{18}\text{O}$  slope demonstrates that if evaporation is the explanation for the enrichment, it must occur in a humid ( $> 95\%$  relative humidity) environment (Gonfiantini, 1986). Sites with slopes of the  $\delta^2\text{H}$  vs.  $\delta^{18}\text{O}$  regression  $> 6.8$  are distinguished in Fig. 5. Fig. 6 demonstrates that they show a spatial clustering, with no relationship to drip classification (Table 1).

**Type 2.** Some sites have variable  $\delta^{18}\text{O}$ ,  $\delta^2\text{H}$  vs.  $\delta^{18}\text{O}$  slopes  $< 6.8$  and lower than the LMWL, and more variability between the time-series. Similar to sites with slopes of the  $\delta^2\text{H}$  vs.  $\delta^{18}\text{O}$  regression  $> 6.8$ , drip flow can be continuous or discontinuous and shows large variations when recharge occurs. Drip sites have an isotopic composition of the

**Table 2**

Parameter values estimated by manual calibration and used to generate model simulations shown in Figs. 3 and 7. Parameters not shown were subject to a Monte Carlo analysis and have ranges defined in Fig. 7.

Parameter	Description	Value	Units
$SMD_i$	Initial soil moisture deficit	TAW	mm
$\theta_{FC}$	Field capacity of soil	25	%
$\theta_{WP}$	Wilting point of soil	5	%
$Z_e$	Soil depth subject to evaporative drying	0.1	m
$Z_r$	Rooting depth	0.47	m
$K_c$	Crop coefficient	1	–
$p$	RAW to TAW ratio	0.5	–
$B$	Proportion of bare soil	0.1	–
$S1\delta_0$	Initial $\delta^{18}\text{O}$ of soil store	–4	‰
$S2\delta_0$	Initial $\delta^{18}\text{O}$ of karst store	–4	‰

water which subsequently becomes heavier, even during periods of drip flow recession, with greater variability and enrichment of  $\delta^{18}\text{O}$  than sites with slopes of the  $\delta^2\text{H}$  vs.  $\delta^{18}\text{O}$  regression  $> 6.8$ . Sites are distinguished by their slope (5.8–6.8, 4.8–3.8, and  $< 3.8$ ) in Fig. 5 and spatial distribution in Fig. 6.

**Type 3.** One site has a low variability of  $\delta^{18}\text{O}$  and a mean composition that is heavier than the weighted mean of precipitation. It can be hypothesised that these sites have a relatively homogenised water source that has undergone isotopic enrichment. Only one such sample is present in our monitoring network, Site 319 (Figs. 5, 6).

Combined isotope and drip rate data demonstrate that the drip water isotopic composition can be explained by the following processes:

- (1) A flow path where the resultant drip water has an initial isotopic composition that reflects the previous infiltration event, and which becomes increasingly isotopically heavy over time but falls on the LMWL. We hypothesise that this is water stored within the shallow unsaturated zone in which evaporation occurs, as observed in laboratory environments (e.g. Ingraham and Criss, 1993). The evaporation has to occur in an environment where  $\text{RH} > 95\%$ , which enriches the isotopic composition close to the LMWL (Gonfiantini, 1986). For this to occur, the store has to be near-surface, to experience diurnal temperature changes necessary for continued evaporation. While allowing sufficient vapour transport to keep driving the evaporative process, it must also be relatively enclosed to permit continual drainage of evaporated (increasingly enriched) water whilst maintaining a high humidity. Although previously unreported as an isotopic process in karst, such a mechanism is possible in hot continental climates which experience large diurnal temperature variations; soil temperature variations lagged from the atmospheric temperature variations could drive circulation of air in and out of the soil/karst voids. The spatial clustering of these sites (slopes of the  $\delta^2\text{H}$  vs.  $\delta^{18}\text{O}$  regression larger than 6.8 in Fig. 6) suggests discrete water stores where evaporation is occurring.
- (2) A flow path similar to (1) above, but where water also experiences evaporative enrichment at lower relative humidity. For this to occur, the air-filled part of the store could be larger, or better ventilated, or the enrichment could occur within a subsequent cave void if infiltration rates are low and relative humidity low. These sites have slopes of the  $\delta^2\text{H}$  vs.  $\delta^{18}\text{O}$  regression of  $< 6.8$  in Fig. 4.

Most infiltration sites comprise a mixture of these two end-member scenarios. For all drip sites combined, the slope correlates with the individual drip water isotope  $\delta^2\text{H}$  vs.  $\delta^{18}\text{O}$  correlation ( $r = 0.92$ ), as noted previously. The strong association between the

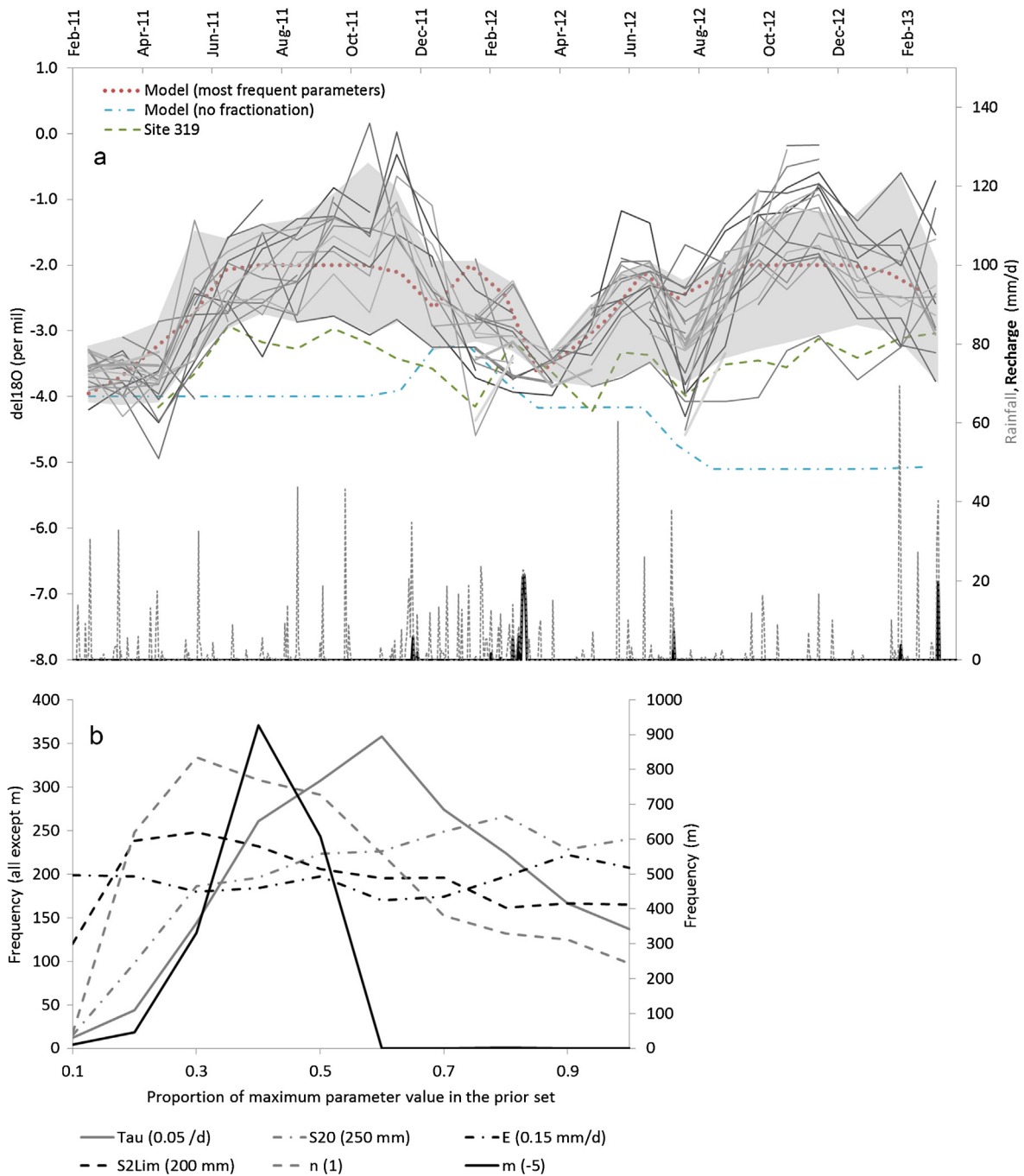


**Fig. 7.** (a) Results from Monte Carlo modelling of drip water compositions shown against observations (solid lines, except dashed Site 319), and observed rainfall and modelled groundwater potential recharge. Shaded area represents the isotopic distribution of the physically plausible model results (1927 out of 50 000). The model output for the most frequently used parameter values are highlighted (dots) and for no karst evaporation/fractionation (dash-dotted) (b) Frequency distributions of the posterior parameter sets, normalised across the range of prior parameter values. Each parameter was free to vary between zero and the value defined in brackets. For example,  $m$  was free to vary randomly between 0 and  $-5$  but most models that had a reasonable fit have values of around  $-2$ . The parameters are the recession constant, the initial value of store S2, evaporative flux from store S2, the S2 store threshold for evaporative fractionation to occur, the empirical constants  $n$ , the empirical constant  $m$ .

slope of the  $\delta^2\text{H}$  vs.  $\delta^{18}\text{O}$  regression at a drip site and the strength of correlation between  $\delta^2\text{H}$  vs.  $\delta^{18}\text{O}$  (Table 1) suggests that the single,  $\text{RH} > 95\%$  evaporation end-member is the primary source of fractionation, with some drips experiencing additional fractionation at lower RH.

### 3.3. Modelled flow and water isotopes

Figs. 3 and 7 show the modelled karst potential groundwater recharge flux indicating that the combined SMB-karst model cap-

tures the timing of the main drip water events well. Calibrated model parameters are shown in Table 2.

The model is able also to simulate the observed patterns and magnitudes of the drip water isotopic composition using the parameters given in Table 2 and Fig. 5. The set of physically plausible models, despite being ‘free’ to vary within the entire range of observable drip composition for Types 1–3 identified above, included no models which consistently maintained  $\delta^{18}\text{O}$  values as low as Site 319, of Type 3. This suggests that the ‘single karst store’ model structure works well for Types 1 and 2 thus supporting our

conceptual model. For Type 3, a mixed source of water is needed, derived from more than one store and so to successfully simulate such sites would require a modification of the existing numerical model to a more complex model structure.

If the karst evaporative process is 'switched off' (Fig. 7) the modelled isotopic drip water reverts to lighter values which vary little from the mean rainwater isotopic composition. This shows that the observed drip water isotopic variations cannot simply be explained by transformation of the input precipitation signal using a standard model of soil and shallow karst processes. It is thus strongly indicative of evaporative equilibrium fractionation (i.e. at conditions >95% RH) in the karst being the dominant mechanism controlling the observed isotopic drip water compositions. Although the evaporative process is modelled empirically it has a sound theoretical basis with Eq. (10) being of the form suggested by Gonfiantini (1986, Eq. (7), p. 117). In the present case the variable  $f$  changes not only due to evaporative loss but also due to drainage from the karst store. Hence, a direct comparison between our parameters  $n$  and  $m$ , and Gonfiantini's  $A$  and  $B$  parameters cannot be made without further (laboratory) investigation to determine the precise form this relationship should take. The values of the physically based parameters retained in the posterior set are physically plausible and lend insight into the potential properties of the karst unsaturated zone at the field site. Most parameters have clearly defined optima for example  $\tau \approx 0.03/\text{d}$ ,  $S2_{lim} \approx 60$  mm and  $S2_0 \approx 200$  mm. The relatively large initial value for  $S2_0$  is suggestive of a period of substantial recharge occurring just prior to the drip isotope monitoring period. This is consistent with high observed drip rates from the site in late 2010, observed prior to cave flooding (Jex et al., 2012). Furthermore, the ranges of  $S2$  and the drainage function,  $\tau$ , are also reasonable in comparison to other karst models (for example, Bradley et al., 2010). The model is relatively insensitive to the evaporation flux (which was set to a maximum of 0.15 mm/d, constrained by our in-cave evaporation rate at Site 1) in determining the timing of the positive isotopic value excursions since the optimum  $S2_{lim}$  values are relatively large in comparison. Hence the isotopic composition is primarily controlled by the empirical  $m$  and  $n$  parameters which control the fractionation of the karst store as it loses water by drainage and evaporation and which have very clearly defined parameter optima at  $n \approx 0.3$ ,  $m \approx -2$ .

The way the model is structured, the rate of fractionation is explicitly dependent on the fraction of water remaining in a shallow karst store. However, since the modelled drip rates are directly proportional to the size of this store (via the recession constant), the fractionation is thus also proportional to the drip rate, below a threshold value. Such a flow rate-dependent evaporative process has recently been directly observed during film flow over a speleothem-forming feature in the shallower part of the Cathedral Cave system. This could also be responsible for the fractionation observed in the deeper South Passage samples reported here. Furthermore, additional evaporative fractionation could occur within the cave passage, especially at low drip rates, either on the stalactite or on the sample collection bottle prior to collection below the paraffin seal (Dreybrodt and Deininger, 2013). However, the high relative humidity in South Passage, and lack of observed relationship between drip rate, drip classification and oxygen isotopic composition, suggests that these effects would be limited, at least at site 2.

It is notable that the recharge events which reset the isotopic composition of the karst store and drip waters in South Passage occur on timescales of hours to days and time-steps of this order of magnitude are needed to predict their occurrence. It is well known that soil moisture balance models are very sensitive to the choice of time-stepping (Howard and Lloyd, 1979). However, most climate models operate on monthly or coarser time-steps and, when

coupled with hydrologic models, structural errors such as those due to time-stepping within a soil-moisture accounting algorithm are rarely considered (Holman et al., 2012). Our results therefore have significant implications for how to model adequately the effect of climate change, for example variations in rainfall intensification, on recharge and speleothem-forming processes in karst environments.

### 3.4. Implications for speleothem records

Our results inform the climatic interpretation of speleothem records in the arid and semi-arid environment in Australia and elsewhere. We have shown that drip water may be enriched by several ‰ owing to evaporative processes; this is of similar magnitude, but opposite in direction, to the fractionation predicted by the estimated atmospheric cooling of up to 9 °C at the Last Glacial Maximum in continental Australia (Galloway, 1965; Miller et al., 1997). Thus if both processes are happening concurrently the speleothem signal could be confounded and affect the imprint of atmospheric temperature in the speleothem record (Fairchild and Baker, 2012). Additionally, we expect that the speleothem isotopic record from these environments may exhibit a considerable range in isotopic values driven by shifts in the frequency–magnitude relationships of infiltration events. This may be recorded on an event-scale but, more relevant to the detection in speleothem isotopic records, is the decadal-centennial timescale on which recharge will be influenced by variability in the dominant climate modes over Australia and more generally in other semi-arid and arid areas globally. Variability in climate modes on these timescales has been observed in proxy records in the Australian region (e.g. Van Ommen and Morgan, 2010). Finally, we draw a link between these results and previous studies that have demonstrated a sensitivity between the timing of speleothem growth and the P–ET balance. Speleothems 'switching on' during cooler time periods (the Last Glacial Maximum and stadial periods) is attributed to reduced evaporation in southern Australia's arid margin (Ayliffe et al., 1998; Cohen et al., 2011). The results of our study may inform the interpretation of speleothem isotopic records from this region as the water balance changes within stadial and glacial events.

## 4. Conclusions

Groundwater recharge in semi-arid environments is episodic; the initial isotopic composition of recharge reflects the isotopic composition of the few rainfall events which are large enough to overcome existing soil moisture deficits. This initial isotopic composition may be affected by subsequent evaporation. At our monitoring site, observed drip waters had a mean  $\delta^{18}\text{O}$  up to 2.77‰ heavier than the weighted mean of precipitation. Here, evaporation from a partially air-filled water store in a high humidity environment is an important process. Our modelling approach demonstrated that this isotope enrichment had to include evaporation from a shallow subsurface karst water store, such as a solutionally widened fracture or proto-cave. The degree of enrichment would be site specific, and dependent on the relative size of the store and its climatic properties (temperature variability, relative humidity), its drainage rate and the time between infiltration events. We have identified and modelled unsaturated zone evaporation as an important process in determining infiltration water  $\delta^{18}\text{O}$  for the first time. We propose that at other caves in semi-arid to arid regions, evaporation will also be a likely source of isotope enrichment, but this requires confirmation.

At Cathedral Cave, infiltration  $\delta^{18}\text{O}$  is a complex function of (1) the isotopic composition of recharge water, (2) the time since the last recharge event (3) water store climate and physical properties

and (4) water flow routing from the store to the drip site, including evaporation during the degassing process that forms speleothems (Dreybrodt and Deininger, 2013). This makes the interpretation of individual stalagmite  $\delta^{18}\text{O}$  records potentially complex. The range of mean drip water  $\delta^{18}\text{O}$  between sample sites gives an indication of this hydrological uncertainty: in our case this is 1.94‰ (mean from  $-1.51\text{‰}$  to  $-3.45\text{‰}$ ). This is greater than the total range of hydrological uncertainty in stalagmite  $\delta^{18}\text{O}$  currently modelled for both modern (Baker and Bradley, 2010; Bradley et al., 2010; Treble et al., 2013), historical (Jex et al., 2013), and Last Glacial Maximum (Baker et al., 2013) environments: all use hydrology modelling approaches that exclude unsaturated zone evaporation as a process.

Interpretation of speleothem  $\delta^{18}\text{O}$  archives, typically from temperate, sub-alpine or cool climates, is one where evidence is presented either (1) for speleothem deposition that is at or close to equilibrium, or (2) that deposition has occurred out of equilibrium, such that kinetic fractionation has occurred (Fairchild and Baker, 2012). The relevant processes in these environments are relatively well observed (e.g. Spötl et al., 2005; Lachniet, 2009) and modelled (Dreybrodt and Scholz, 2011). However, in semi-arid to arid environments, subject to surface, soil and unsaturated zone evaporation, our understanding of the interpretation of speleothem  $\delta^{18}\text{O}$  is still developing. In this study, we attribute at least part of the observed  $\delta^{18}\text{O}$  isotope composition of stalagmite forming drip waters to evaporation in the unsaturated zone, and propose that this process is likely to occur at other sites where  $\text{ET} > \text{P}$ , such as those reported in central Texas (Pape et al., 2010). Thus, interpretation of stalagmite  $\delta^{18}\text{O}$  in these regions could be a function of this process, as well as the previously recognised within-cave processes such as kinetic effects (due to the differing rate constants of calcite precipitation for the heavy and light isotopes; Dreybrodt, 2008; Dreybrodt and Scholz, 2011) and evaporation during degassing (Dreybrodt and Deininger, 2013). As well as having relevance to the interpretation of speleothem records from modern day regions where  $\text{ET} > \text{P}$  and infiltration is infrequent, our findings are also relevant to the interpretation of Quaternary speleothem records from regions where the modern day climate is temperate or Mediterranean, but in the past experienced some degree of aridity.

## Acknowledgements

CJ, AB, MSA and RIA were supported the NCGRT, PG by the NSW Science Leveraging Fund and MOC by the European Community's Seventh Framework Programme [FP7/2007–2013] under grant agreement No. 299091. Groundwater infrastructure used by the research team was funded by the Australian Government Groundwater Education Investment Fund and weather station data downloaded from (<http://groundwater.anu.edu.au>). We thank Monika Markowska for provision of South Passage temperature data and Even Jensen and Gabriel Rau for provision of relative humidity data, Wellington Council for permission to work at the Wellington Caves site, and Chris George, Col Birchall, Mike Augee and staff at Wellington Caves that made this research possible. The reviews of Darrel Tremaine and two anonymous reviewers greatly improved the clarity of the manuscript.

## Appendix A. Supplementary materials

Rainfall double mass plots, isotope and drip rate data are available on-line at <http://dx.doi.org/10.1016/j.epsl.2014.03.034> as supplementary spreadsheets.

## References

- Allison, G.B., 1982. The relationship between  $^{18}\text{O}$  and deuterium in water in sand columns undergoing evaporation. *J. Hydrol.* 55, 163–169.
- Allison, G.B., Hughes, M.W., 1983. The use of natural tracers as indicators of soil-water movement in a temperate semi-arid region. *J. Hydrol.* 60, 157–173.
- Allison, G.B., Barnes, C.J., Hughes, M.W., 1983. The distribution of deuterium and  $^{18}\text{O}$  in dry soils. 2 Experimental. *J. Hydrol.* 64, 377–397.
- Allison, G.B., Colin-Kaczala, C., Filly, A., Fontes, J.Ch., 1987. Measurement of isotopic equilibrium between water, water vapour and soil  $\text{CO}_2$  in arid zone soils. *J. Hydrol.* 95, 131–141.
- Allen, R.G., Pereira, L.S., Raes, D., Smith, M., 1998. *Crop Evapotranspiration – Guidelines for Computing Crop Water Requirements*. FAO Irrig. Drain. Pap., vol. 56. FAO, Rome, Italy.
- Ayliffe, L.K., Marianelli, P.C., Moriarty, K.C., Wells, R.T., McCulloch, M.T., Mortimer, G.E., Hellstrom, J.C., 1998. 500 ka precipitation record from southeastern Australia: evidence for interglacial relative aridity. *Geology* 26, 147–150.
- Baker, A., Brunson, C., 2003. Non-linearities in drip water hydrology: an example from Stump Cross Caverns, Yorkshire. *J. Hydrol.* 277, 151–163.
- Baker, A., Bradley, C., 2010. Modern stalagmite  $\delta^{18}\text{O}$ : instrumental calibration and forward modelling. *Glob. Planet. Change* 71, 201–206.
- Baker, A., Bradley, C., Phipps, S.J., 2013. Hydrological modelling of stalagmite  $\delta^{18}\text{O}$  response to glacial–interglacial transitions. *Geophys. Res. Lett.* 40 (12), 3207–3212.
- Barnes, C.J., Allison, G.B., 1988. Tracing of water movement in the unsaturated zone using stable isotope of hydrogen and oxygen. *J. Hydrol.* 100, 143–176.
- Beven, K., Binley, A., 1992. The future of distributed models: model calibration and uncertainty prediction. *Hydrol. Process.* 6, 279–298.
- Blyth, A.J., Jex, C., Baker, A., Khan, S.J., Schouten, S., 2014. Contrasting distributions of glycerol dialkyl glycerol tetraethers (GDGTs) in speleothems and associated soils. *Org. Geochem.* 69, 1–10.
- Bradley, C., Baker, A., Jex, C., Leng, M.J., 2010. Hydrological uncertainties in the modelling of cave drip-water  $\delta^{18}\text{O}$  and the implications for stalagmite palaeoclimate reconstructions. *Quat. Sci. Rev.* 29, 2201–2214.
- Cohen, T.J., Nanson, G.C., Jansen, J.D., Jones, B.G., Jacobs, Z., Treble, P., Price, D.M., May, J.H., Smith, A.M., Ayliffe, L.K., Hellstrom, J.C., 2011. Continental aridification and the vanishing of Australia's megalakes. *Geology* 39, 167–170.
- Cuthbert, M.O., Mackay, R., Nimmo, J.R., 2013. Linking soil moisture balance and source-responsive models to estimate diffuse and preferential components of groundwater recharge. *Hydrol. Earth Syst. Sci.* 17, 1003–1019.
- Dreybrodt, W., 2008. Evolution of the isotopic composition of carbon and oxygen in a calcite precipitating  $\text{H}_2\text{O}-\text{CO}_2-\text{CaCO}_3$  solution and the related isotopic composition of calcite in stalagmites. *Geochim. Cosmochim. Acta* 72, 4712–4724.
- Dreybrodt, W., Scholz, D., 2011. Climatic dependence of stable carbon and oxygen isotope signals recorded in speleothems: from soil water to speleothem calcite. *Geochim. Cosmochim. Acta* 75, 734–752.
- Dreybrodt, W., Deininger, M., 2013. The impact of evaporation to the isotope composition of DIC in calcite precipitating water films in equilibrium and kinetic fractionation models. *Geochim. Cosmochim. Acta*. <http://dx.doi.org/10.1016/j.gca.2013.10.004>.
- Fairchild, I.J., Baker, A., 2012. *Speleothem Science*. Wiley–Blackwell.
- Galloway, R.W., 1965. Late quaternary climates in Australia. *J. Geol.* 73, 603–618.
- Gonfiantini, R., 1986. Environmental isotopes in lake studies. In: Fritz, P., Fontes, J.Ch. (Eds.), *Handbook of Environmental Isotope Geochemistry*, vol. 2: The Terrestrial Environment. Elsevier, pp. 113–168.
- Holman, I.P., Allen, D.M., Cuthbert, M.O., Goderniaux, P., 2012. Towards best practice for assessing the impacts of climate change on groundwater. *Hydrogeol. J.* 20, 1–4.
- Howard, K.W.F., Lloyd, J.W., 1979. The sensitivity of parameters in the Penman evaporation equations and direct recharge balance. *J. Hydrol.* 41 (3), 329–344.
- Ingraham, N.L., Chapman, J.B., Hess, J.W., 1990. Stable isotopes in cave pool systems: Carlsbad Cavern, New Mexico, USA. *Chem. Geol.* 86, 65–74.
- Ingraham, N.L., Criss, R.E., 1993. Effect of surface area and volume on the rate of isotopic exchange between water and water vapour. *J. Geophys. Res.* 98 (D11), 20547–20553.
- Jex, C.N., Mariethoz, G., Baker, A., Graham, P., Andersen, M.S., Acworth, I., Edwards, N., Azcurra, C., 2012. Spatially dense drip hydrological monitoring and infiltration behaviour at the Wellington Caves, South East Australia. *Int. J. Speleol.* 41 (2), 285–298.
- Jex, C.N., Phipps, S.J., Baker, A., Bradley, C., 2013. Reducing uncertainty in the climatic interpretations of speleothem  $\delta^{18}\text{O}$ . *Geophys. Res. Lett.* 40, 2259–2264.
- Lachniet, M.S., 2009. Climatic and environmental controls on speleothem oxygen-isotope values. *Quat. Sci. Rev.* 28, 412–432.
- Lis, G., Wassenaar, I.L., Hendry, M.J., 2007. High-precision laser spectroscopy D/H and  $^{18}\text{O}/^{16}\text{O}$  measurements of microliter natural water samples. *Anal. Chem.* 80, 287–293.
- Mariethoz, G., Baker, A., Sivakumar, B., Hartland, A., Graham, P., 2012. Chaos and irregularity in karst percolation. *Geophys. Res. Lett.* L23305.
- Miller, G.H., Magee, J.W., Jull, A.J.T., 1997. Low-latitude glacial cooling in the Southern Hemisphere from amino-acid racemisation in emu eggshells. *Nature* 385, 241–244.

- McDonald, J., Drysdale, R., Hill, D., Chisari, R., Wong, H., 2007. The hydrochemical response of cave drip waters to sub-annual and inter-annual climate variability, Wombeyan Caves, SE Australia. *Chem. Geol.* 244, 605–623.
- Osborne, R.A.L., 2007. Cathedral Cave, Wellington Caves, New South Wales, Australia. A multiphase, non-fluvial cave. *Earth Surf. Process. Landf.* 32, 2075–2103.
- Osborne, R.A.L., 2010. Rethinking eastern Australian caves. *Geol. Soc. (Lond.) Spec. Publ.* 346, 289–308.
- Pape, J.R., Banner, J.L., Mack, L.E., Musgrove, M., Guilfoyle, A., 2010. Controls on oxygen isotope variability in precipitation and cave drip waters, central Texas, USA. *J. Hydrol.* 385, 203–215.
- Rutledge, H., Baker, A., Marjo, C., Andersen, M.S., Graham, P.W., Cuthbert, M.O., Rau, G.C., Roshan, H., Markowska, M., Mariethoz, G., Jex, C., 2014. Dripwater organic matter and trace element geochemistry in a semi-arid karst environment: implications for speleothem paleoclimatology. *Geochim. Cosmochim. Acta*. <http://dx.doi.org/10.1016/j.gca.2014.03.036>.
- Sonntag, C., Christmann, D., Munnich, K.O., 1985. Laboratory and field experiments on infiltration and evaporation of soil water by means of deuterium and oxygen-18. In: *Proc. IAEA/GSF Meeting, Vienna, 1984*. In: IAEA-Tecdoc, vol. 357, pp. 145–159.
- Spötl, C., Fairchild, I.J., Tooth, A.F., 2005. Cave air control on dripwater geochemistry, Obir caves (Austria): implications for speleothem deposition in dynamically ventilated caves. *Geochim. Cosmochim. Acta* 69, 2451–2468.
- Treble, P.C., Bradley, C., Wood, A., Baker, A., Jex, C.N., Fairchild, I.J., Gagan, M.K., Cowley, J., Azcurra, C., 2013. An isotopic and modelling study of flow paths and storage in Quaternary calcarenite, SW Australia: implications for speleothem paleoclimate records. *Quat. Sci. Rev.* 64, 90–103.
- Van Ommen, T.D., Morgan, V., 2010. Snowfall increase in coastal East Antarctica linked with southwest Western Australian drought. *Nat. Geosci.* 3, 267–272.
- Wassenaar, L.I., Hendry, M.J., Chostner, V.L., Lis, G.P., 2008. High Resolution Pore Water  $\delta^2\text{H}$  and  $\delta^{18}\text{O}$  measurements by  $\text{H}_2\text{O}$  (liquid)– $\text{H}_2\text{O}$  (vapor) equilibration. *Environ. Sci. Technol.* 2008 (42), 9262–9267.